Cobalt Loading Effects on the Physico-Chemical Properties and Performance of Co Promoted Alkalized MoS_2/CNTs Catalysts for Higher Alcohols Synthesis

Tavasoli, Ahmad*+; Karimi, Saba; Zolfaghari, Zahra; Taghavi, Somayeh; Amirfirouzkouhi, Hamideh; Babatabar, Mokhtar

School of Chemistry, College of Science, University of Tehran, Tehran, I.R. IRAN

ABSTRACT: *An extensive study of Higher Alcohol Synthesis (HAS) from synthesis gas using cobalt (Co) promoted alkalized MoS_2 catalysts supported on Carbon NanoTubes (CNTs) is reported. Up to 5wt.% of Co is added to the 15wt.% Mo-8wt.%K/ CNTs by incipient wetness impregnation method. Most of the metal particles were homogeneously distributed inside the tubes and the rest on the outer surface of the CNTs. The catalysts are extensively characterized by different methods and the activity and selectivity of the catalysts were assessed in a fixed bed micro-reactor. Temperature Programmed Reduction (TPR) tests showed that addition of cobalt decreased the second TPR peak temperature from 801 to 660°C. The diffraction peaks that represent the characteristic K-Mo-O phase (i.e. $K_2Mo_2O_7$, K_2MoO_4, $K_2Mo_7O_{20}$, KMo_4O_6, and $K_{0.33}MoO_3$; these species can enhances formation of higher alcohols) were observed in the X- Ray Diffraction (XRD) patterns of unpromoted Mo-K/CNTs and to a greater extent in the XRD patterns of Co-promoted Mo-K/CNTs catalysts. Co addition to Mo-K/CNTs not only increased the number of surface sites, but also decreased the average active metal particle sizes from 7.53 to 5.33 nm and increased the percentage dispersion from 51.1 to 68.2%. Among the catalysts with different Co loadings, catalyst with 5 wt.% Co showed the highest %CO conversion of 38.8%. The total alcohol selectivity reached a maximum of 59.7 wt.% on the catalyst promoted with 3 wt.% cobalt. The catalyst with 3 wt.% Co exhibited selectivity of 41.65 wt.% towards higher alcohols.*

KEY WORDS: *Higher alcohols synthesis, Molybdenum, Cobalt, Carbon nanotubes, Physicochemical properties, Activity, Selectivity.*

INTRODUCTION

Higher Alcohols Synthesis (HAS) from CO hydrogenation, as one of the most promising processes for coal, natural gas and biomass conversions to synthetic fuels, is receiving a renewed interest for both industrial and academic applications because of the emergency of transportation fuel shortage in the whole world. As a result, several catalytic systems for HAS, including the MoS_2-based catalysts, Rh-based catalysts, modified

* *To whom correspondence should be addressed.*
+ *E-mail: tavassolia@khayam.ut.ac.ir*
1021-9986/13/1/ 9/$/2.90

Table 1: Textural properties of the supports.

Sample	BET surface area (m^2/g)	Total pore volume (mL/g)	Average pore diameter (Å)	% metals
Fresh CNTs	209.01	0.48	91.62	0.60%
30% HNO_3 Treated CNTs	252.59	0.59	94.12	0%

methanol synthesis catalysts and modified Fischer-Tropsch catalysts were developed [1-5].

Supported molybdenum sulfide (MoS_2) based catalysts are the most attractive higher alcohols synthesis catalysts due to their excellent resistance to sulfur poisoning and high activity for the water-gas shift reaction [6-10]. Molybdenum sulfide catalysts mainly produce hydrocarbons but, when they get promoted with alkali metals,they can produce alcohols [11, 12]. The function of alkali metal is to reduce the hydrogenation ability of alkyl species to form alkanes and increase the sites active for formation of alcohols [13]. Also, cobalt is used as promoter in supported molybdenum sulfide catalysts [14-17]. It has been suggested that addition of cobalt to MoS_2 catalysts increases the yield of ethanol and higher alcohols [14-17]. However, the most favorable amount of cobalt that optimizes the rate of higher alcohols synthesis using cobalt promoted MoS_2 catalysts, has not been determined.

The use of carbon as catalysts support has been drawing attention, due to their flexibility in tailoring the catalyst properties to specific needs. Activated carbon has many advantages if utilized as catalyst support (resistance to acidic or basic media, stable at high temperatures, etc.). Carbon nanotubes possess similar properties and in most cases outperform activated carbon in this respect. Carbon nanotubes with unique properties such as uniform pore size distribution, meso and macro pore structure, inert surface properties, highly graphitized tube-walls, sp^2-C-constructed surfaces and resistance to acid and base environment can play an important role in a large number of catalytic reactions. It is anticipated that using mesoporous structured carbon nanotubes improve the catalytic performance [18-23].

In our previous work, we extensively studied the activity and product selectivity of CNTs supported potassium promoted molybdenum sulfide catalysts [23]. In the present work, we intend to enhance the activity and selectivity of the CNTs supported alkalized molybdenum sulfide catalyst using optimum amount of cobalt as MoS_2 catalyst promoter.

EXPERIMENTAL SECTION

Catalyst preparation

Multi wall CNTs (purity >95%) (Characteristics are shown in Table 1) were used as support for preparation of the catalysts. Prior to impregnation the support was treated with 30% HNO_3 reflux at 120˚C overnight, washed with distilled water several times and dried at 120˚C for 6h. All the catalysts were prepared by the incipient wetness impregnation with aqueous solutions of $(NH_4)6Mo_7O_{24}.4H_2O$, K_2CO_3 and $Co(NO_3)_2.6H_2O$. First, the support was impregnated with Mo precursor, followed by drying at 120˚C for 6h and calcination in argon flow of 50 ml/min for 4h at 450˚C with a heating rate of 10˚C/min [19-22]. Then it was impregnated with an aqueous solution of K_2CO_3 and dried and calcined at the same conditions of the last step. Finally, it was impregnated with aqueous solution of $Co(NO_3)_2.6H_2O$. After 3rd impregnation step, the catalysts dried and calcined similar to the last two steps. Six catalysts were prepared with different loadings of cobalt (0, 1, 2, 3, 4, and 5 wt.%), 15 wt.% molybdenum and 8 wt.% potassium.

ICP-OES

The metal loadings of fresh and acid treated supports (impurities) and molybdenum, potassium and cobalt loadings of the calcined catalysts were performed using Varian VISTA-MPX Inductively Coupled Plasma-Optical Emission Spectrometry (ICP-OES) instrument.

BET surface area measurements/BJH pore size distributions

Surface area, pore volume and average pores diameter of the fresh and acid treated supports were measured using an ASAP-2010 V2 Micrometrics system. The samples were degassed at 200˚C for 4h under 50 mTorr vacuums and their BET area, pore volume and pore diameter was determined.

X-ray diffraction

The phases and particle sizes of the crystals present in all the catalysts were analyzed by XRD using a Philips

Analytical X-ray diffractometer (XPert MPD) with monochromatized Co/Kα radiation, 2θ angles from 20˚ to 80˚. The Debye–Scherer formula ($d = 0.9\lambda/\beta\cos\theta$, where β is FWHM (Full Width at Half Maximum), λ is wave length of X-ray, 0.9 is a constant) was applied to MoO_3 peaks at 2θ = 43.3, in order to calculate the average particle sizes.

Transmission Electron Microscopy (TEM)

The morphology of the catalysts was characterized by Transmission Electron Microscopy (TEM). Sample specimens for TEM studies were prepared by ultrasonic dispersion of the catalysts in ethanol, and the suspensions were dropped onto a carbon-coated copper grid. TEM investigations were carried out using a Philips CM20 (100 kV) transmission electron microscope equipped with a NARON energy-dispersive spectrometer with a germanium detector.

Temperature Programmed Reduction (TPR)

The H_2-TPR profiles of the catalysts were performed in order to study the reducibility of the metal species in the catalysts. The catalyst sample (0.05g) was first purged in a flow of Helium at 140˚C to remove traces of water and gases exist in catalyst, and then cooled to 40˚C. Then the TPR of each sample was performed using 5% H_2 in Ar stream at a flow rate of 40 mL/min at atmospheric pressure using Micrometrics TPD-TPR 2900 analyzer equipped with a Thermal Conductivity Detector (TCD), heating at a linearly programmed rate of 10˚C/min up to 850˚C.

Hydrogen chemisorption

The amount of chemisorbed hydrogen was measured using the Micrometrics TPD-TPR 2900 analyzer system. 0.2 g of the calcined catalyst was first purged in a flow of argon at 140°C to remove traces of water. The temperature was then raised to 500°C at a linearly programmed rate of 10°C/min and catalyst was reduced for 12h under hydrogen flow and then cooled to 40°C. Then the flow of hydrogen was switched to argon for 30 min in order to remove the weakly adsorbed hydrogen. Afterwards the Temperature Programmed Desorption (TPD) of the samples was performed by increasing the temperature of the samples, with a ramp rate of 40°C/min, to 500°C under the argon flow. The TPD spectrum was used to determine the dispersion and average particle size.

Reaction setup and test procedure

Higher alcohol synthesis been performed in a tubular down flow, fixed-bed reactor system. The reactor was made up of Inconel tube of 450-mm length and 22-mm inside diameter. The reactor temperature was controlled via a PID temperature controller. Brooks 5850 mass flow controllers were used to add H_2 and CO at the desired rate to the reactor. The reactor was packed with 0.5 g of catalyst diluted with 90-mesh size silicon carbide and housed in a melted salt bath controlled by a temperature controller. The reactor was pressurized to 30 bars with He and the sulfurization as well as the reduction was carried out for 6 h at 450˚C at a heating rate of 2˚C/min using gas mixture containing 5 mol% H_2S in H_2 and flow rate of 50 mL/min. The temperature was then lowered to the reaction temperature, and the system was then pressurized to the reaction condition. The feed gas mixture (H_2/CO ratio of 2) was passed through mass flow controllers and the HAS reaction was carried out at steady state under the reaction conditions of 320˚C, 70 bars, and gas hourly space velocity of 3.6 nL/g catal./h over a period of 24h. The product gas was cooled to 0˚C and separated into gas and liquid phases at the reaction pressure. The CO conversion and other gaseous products were monitored with time intervals of 1h. The products were collected after completion of the run and analyzed by means of three gas chromatographs, a Shimadzu 4C gas chromatograph equipped with two subsequent connected packed columns: Porapak Q and Molecular Sieve 5Å, and a Thermal Conductivity Detector (TCD) with argon which was used as a carrier gas for hydrogen analysis. A Varian CP 3800 with a chromosorb column and a Thermal Conductivity Detector (TCD) were used for CO, CO_2, CH_4 and other non-condensable gases. A Varian CP 3800 with a Petrocol Tm DH100 fused silica capillary column and a Flame Ionization Detector (FID) were used for organic liquid products so that a complete product distribution could be provided.

RESULTS AND DISCUSSION

Characterization overview

Textural properties of the fresh and acid treated carbon nanotubes are given in the Table 1. The data indicate that in the case of acid-washed support, surface area, total pore volume and average internal diameter of nanotubes increased significantly which will result

Table 1: Chemical composition of CNTs supported Mo-K-Co catalysts.

Catalyst	Targeted composition (wt.%)			Measured composition (wt.%)		
	Mo	K	Co	Mo	K	Co
C_1	15	8	0	14.7	7.9	0
C_2	15	8	1	14.7	7.9	0.97
C_3	15	8	2	14.7	7.9	1.93
C_4	15	8	3	14.7	7.9	2.9
C_5	15	8	4	14.7	7.9	3.87
C_6	15	8	5	14.7	7.9	4.82

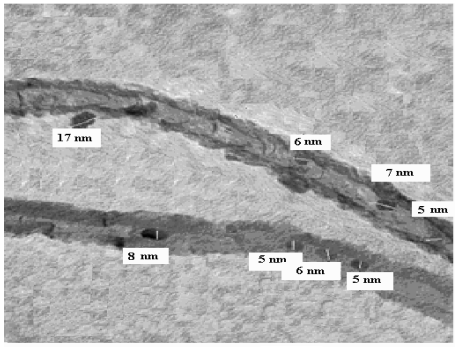

Fig. 1: TEM image of the unpromoted catalyst.

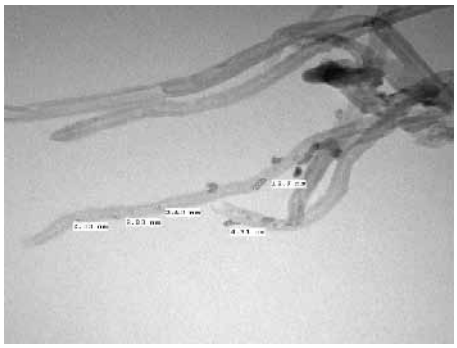

Fig. 2: TEM image of the 3wt.% cobalt promoted catalyst.

in better dispersion of metal as well as enhancement of catalyst activity. Table 1 also shows the metal content for the untreated fresh CNTs and acid treated CNTs (determined by ICP). As shown the amount of encapsulated metal content in the fresh CNTs was about 0.6wt% which decreased to zero for acid treated CNTs.

The elemental compositions of calcined catalysts measured by ICP are given in Table 2. The measured contents of the prepared catalysts are found to be slightly lower compared to the targeted values. The discrepancies may be due to incomplete impregnation of metals.

Figs. 1 and 2 present the TEM images of the unpromoted catalyst and the catalyst promoted with 3wt.% cobalt, respectively. TEM images of both catalysts show that the particles are disturbed inside and outside of the nanotube walls. In the case of unpromoted catalyst, the sizes of particles located inside and outside of the nanotubes are in the range of 3-16 nm. However for the catalyst promoted with 3wt.% cobalt, the sizes of particles are in the rage of 2-13 nm. It seems that addition of cobalt to the carbon nanotubes supported molybdenum oxide catalyst suppressed the growth of molybdenum particles. According to these figures, the average particle size for the 15Mo8K/CNTs and 15Mo8K3Co/CNTs catalysts are 7.1 and 5.6 nm respectively.

To determine the crystalline phases, X-ray diffraction experiments of the catalysts were performed. Fig. 3 presents the XRD spectrum of the unpromoted catalyst and the catalysts with different loadings of cobalt. In the XRD spectrum of the unprompted catalyst the peaks at 2θ values of 43.3, 63.2 and 71.9 corresponds to MoO_3. Also, in the XRD of this catalyst two peaks at 2θ values of 40.4, and 46.3 with weak intensities can be correspond to the crystalline structure of K–Mo-O mixed oxide species ($K_2Mo_2O_7$, K_2MoO_4, $K_2Mo_7O_{20}$, KMo_4O_6, and $K_{0.33}MoO_3$) [13,19-23].

As shown in this figure, addition of cobalt decreases the intensity of MoO_3 peaks. Also this figure shows that, at a fixed Mo loading of 15 wt.%, the intensities of peaks of MoO_3 decreased significantly, when Co loading increased from 1 to 5 wt.% (peaks at 2θ values of 43.3, 63.2 and 71.9). This indicates the fact that Mo dispersion

Table 2: Average particle size for the catalysts (determined by XRD).

Catalyst	dp (nm) (determined by XRD)
C_1	7.5
C_2	6.8
C_3	6.4
C_4	5.8
C_5	5.6
C_6	5.6

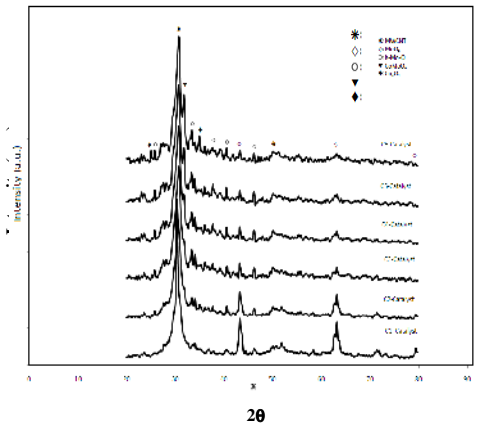

Fig. 3: XRD patterns of the catalysts with different cobalt loadings.

increases with the addition of Co species, leading to smaller molybdenum particles. Table 3 shows the average sizes of MoO_3 particles for the unpromoted catalyst and the catalysts promoted with different amounts of cobalt calculated by Debye–Scherer formula at 2θ = 43.3. As can be seen addition of 3 wt.% Co decreases the crystal diameter of MoO_3 from 7.5 to 5.8 nm. These results are in good agreement with the average particle sizes calculated by TEM (for the unpromoted ant 3wt.% promoted catalysts).

Also in the XRD of the cobalt promoted catalysts, several kinds of K-Mo-O mixed phases with higher intensity exist in oxidized form of the catalysts. Five peaks at 2θ values of 25.8, 33.5, 37.6, 40.4 and 46.3 can be correspond to K-Mo-O mixed oxide species ($K_2Mo_2O_7$, K_2MoO_4, $K_2Mo_7O_{20}$, KMo_4O_6, and $K_{0.33}MoO_3$). This implies that with addition of cobalt to the CNTs supported Molybdenum catalyst; the chemical interactions between K–Mo–O species are increased, enhancing the conditions for the formation of alcohols [19-23]. For the catalysts promoted with 1, 2 and 3wt.% cobalt, no peaks related to the Co species are detected from the XRD spectra of the catalysts in the oxide form, indicating good dispersion of those species on the catalyst. However, when Co loadings increases to 4 and 5wt.%, the peaks of $CoMoO_4$ appear at 2θ values of 31.9 and the peaks of Co_3O_4 come out at 2θ values 25.2 and 34.9. Although formation of K-Mo-O mixed oxides enhances formation of alcohols, cobalt oxide accelerates the formation of hydrocarbons [19-23].

Temperature Programmed Reduction (TPR) tests were performed to determine the reducibility of the calcined catalysts. Fig. 4 shows the TPR spectrum of the unpromoted catalyst and the catalysts containing different amounts of cobalt. The first peak at 506°C in the TPR spectrum of the unpromoted catalyst is typically assigned to the reduction of Mo^{6+} to Mo^{4+}. The second peak at 801°C is mainly assigned to the second reduction step, which is mainly reduction of Mo^{4+} to metallic Mo^o [19-23].

This figure also shows that addition of cobalt to 15Mo8K/CNT catalyst decreases the reduction temperature of the second TPR peak significantly. However the decrease in the first TRP peak temperature is negligible. Cobalt plays a significant role on decreasing the temperature of the second TPR peak temperature for the reduction of Mo^{4+} to metallic Mo^o (addition of 1wt.% cobalt to the 15Mo8K/CNT catalyst decreased the second TPR peak temperature from 801 to 685°C). The reduction of cobalt oxide occurs at temperatures lower (about 640 °C) than that of the Mo^{4+} to metallic Mo^o. It can be concluded that Co enhances the reduction of Mo^{4+}, by spillover of hydrogen from Co to the Mo^{4+} sits. The first step reduction of Mo^{6+} to Mo^{4+} is occurs at about 500-510°C, which explains the lack of cobalt's effect on the first low temperature reduction peak. Fig. 4 also shows that increasing the amount of cobalt loading from 1 to 5wt.%, decreases the second TPR peak temperature from 685 to 660°C. Also H_2 consumption (not shown hear) which is proportional to the percentage reduction of catalyst, increased upon promotion of the catalysts with cobalt.

The results of hydrogen chemisorption tests are given in Table 4. As shown, increasing Co loading from 0 to 5 wt.%, increased the hydrogen uptake, significantly. Percentage dispersion increased from 51.07 to 67.07 upon increasing Co from 0 to 3wt.%. However addition of

Table 4: H_2 chemisorption results for the catalysts.

Catalyst	μ mole H_2 desorbed/ g. cat	% Dispersion	dP (nm)
C_1	399	51.072	7.53
C_2	459	58.752	6.39
C_3	504	64.512	5.69
C_4	524	67.072	5.43
C_5	529	67.712	5.36
C_6	533	68.224	5.31

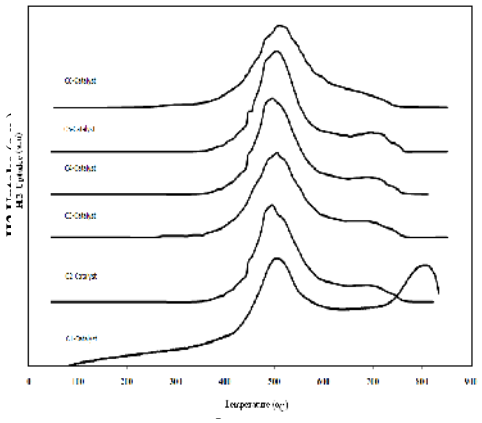

Fig. 4: TPR profiles for the catalysts with different cobalt loadings.

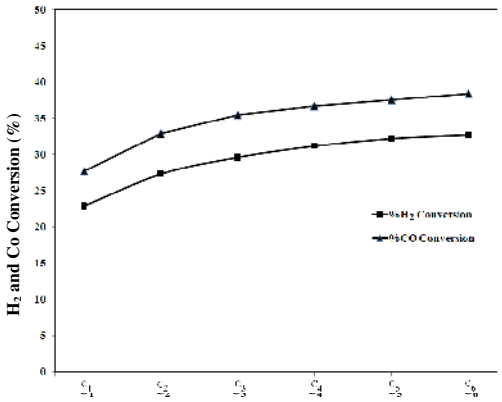

Fig. 5: Percentage H_2 and CO conversion variations with cobalt loadings.

cobalt to 5wt.% increased the percentage dispersion to 68.22%. The particle diameter decreased, which is in agreement with the results of XRD tests. Higher dispersion and smaller molybdenum cluster sizes will increase the number of sites available for CO conversion reactions in cobalt promoted CNTs supported molybdenum catalysts.

Activity and products selectivities results

Synthesis of higher alcohols was carried out after reduction and sulfidation of catalysts in a fixed bed reactor at 320°C, 70 bars, Gas Hourly Space Velocity (GHSV) of 3.6 nL/g cat. h and $H_2/CO=2$. The liquid products were collected at 0°C and the exit gas was analyzed to measure the CO conversion. The analysis of liquid products indicates that methanol, ethanol, n-propanol n-butanol are the major products simultaneously with small amounts of other higher alcohols. The analysis of exit gas indicates that methane and carbon dioxide are the major component apart from CO and H_2.

Table 5 presents the percentage CO and H_2 conversion and different product selectivities during 24 hours of continuous synthesis for unpromoted catalyst. As shown in this table, methanol has the highest product selectivity. The ratio of HA /CH_3OH (higher alcohols to methanol) is about 4/3. It has been suggested that sulfidation of the mixed oxides present in the calcined form of the catalysts and formation of the Mo-K-S species are responsible for the alcohol formation via following CO insertion mechanism [17, 19-23].

$$CO + 2H_2 \leftrightarrow CH_3OH \quad (1)$$

$$CH_3OH + H_2 \rightarrow CH_4 + H_2O \quad (2)$$

$$CH_3OH + CO + 2H_2 \rightarrow C_2H_5OH + H_2O \quad (3)$$

$$C_2H_5OH + CO + 2H_2 \rightarrow C_3H_7OH + H_2O \quad (4)$$

$$CO + H_2O \leftrightarrow CO_2 + H_2 \quad (5)$$

In this mechanism, adsorption of CO and hydrogen takes place at different sites to from intermediate surface species.

Table 5: %CO & %H2 conversions and different product selectivities for unpromoted catalyst.

% Co Conversion	$\%H_2$ conversion	Total alcohols selectivity	Methanol selectivity	Ethanol selectivity	Propanol selectivity	Buthanol and higher alcohols selectivity
27.72	22.89	45.31	19.40	10.25	6.57	9.10

These surface species propagate chain growth through hydrogenation, followed by insertion of molecularly adsorbed CO species to form different long-chain intermediates. The direct hydrogenation of these intermediate hydrocarbon species leads to the formation of hydrocarbon, methanol, and higher alcohols.

Fig. 5 shows the influence of cobalt promoter on the catalytic properties of Mo-K/CNTs catalyst for the synthesis of higher alcohols from synthesis gas. As shown on this figure, the %CO conversion and $\%H_2$ conversion increased from 27.7 to 32.9% and 22.9 to 27.3 with addition of 1 wt.% cobalt to the CNTs-supported 15 wt.% Mo and 8 wt.% K catalyst. The increase in %CO conversion upon addition of 1 wt.% cobalt, can be due to the increase in Mo dispersion (Confirmed by XRD, TEM and H_2 chemisorption tests) and the enhancement in reduction of Mo^{4+} to metallic Mo^o (confirmed by TPR tests). Also, it has been suggested that incorporation of cobalt on edge surfaces on MoS_2 (after catalyst sulfidation) increases the number of active sites, thus significantly increase the activity of the catalyst [19-25]. Also this figure reveals that, increasing cobalt form 1 to 5 wt.%, increased the %CO conversion from 32.9 to 38.4%. Comparing the data of this figure with the data of Table 4 demonstrate that the %CO conversion increases in accordance with the hydrogen uptake, with addition of cobalt loading. The catalyst with 5wt.% Co showed the highest CO conversion of 38.4% and H_2 conversion of 32.7%. It can be concluded that increasing Co loadings from 0 to 5 wt.% increases the active surface area of the catalysts which in turn leads to enhancement of CO and H_2 conversions.

Fig. 6 shows the influence of cobalt promoter on the product selectivities (alcohols and hydrocarbons in liquid products) of the catalysts. As shown, incorporation of 1 wt.% cobalt increased the selectivity of total alcohols in the liquid products from 45.3 to 51.6 wt.% (in the liquid products). As shown by XRD tests, addition of cobalt to the CNTs supported Molybdenum catalyst increases the chemical interactions between K–Mo–O species (enhances formation of $K_2Mo_2O_7$, K_2MoO_4, $K_2Mo_7O_{20}$, KMo_4O_6, and $K_{0.33}MoO_3$) which in turn increases the sites active for higher alcohols formation [19-23]. In addition the increase in the selectivity of total alcohols and the decrease in the selectivity of hydrocarbons can be due to decreased availability of hydrogenation active centers, i.e. MoS_2 species as also confirmed by XRD results (The intensity of peaks corresponding to MoO_3 decreased with addition of cobalt). This figure also shows that increasing the cobalt content of the catalyst from 1 to 3 wt.%, increases the alcohols selectivity from 51.6 to 59.70 wt.%. However, rising the cobalt to 4 and 5 wt.%, decreases the alcohols selectivity to some extent. The results of H_2 chemisorption experiments, showed that the percentage dispersion increases with increasing cobalt content of the catalyst from 1 to 3 wt.% and remains approximately unchanged upon increasing cobalt content to 4 to 5 wt.%. The small particles are more favorable for interactions and formation of K–Mo–O mixed oxides which after sulfidation can act as higher alcohols formation sites. The small decrease in the alcohols selectivity at higher cobalt loadings can be due to the decrease in K–Mo–O mixed oxides formation and particularly due to the unfavorable formation of Co_3O_4 (After sulfidation process will change to Co_9S_8) which accelerates the formation of hydrocarbons [26]. It is to note that the formation of Co_3O_4 confirmed by XRD tests (shown on Fig. 3 for catalysts with cobalt content of 4 to 5 wt.%). It can be concluded that the optimum alcohol selectivity of 59.7 wt.% is attained on the CNT supported catalyst with a cobalt percentage of 3 wt.%.

Fig. 7 shows the selectivity trends of individual alcohols with increased cobalt loadings. As shown, promotion of the 15Mo8K/CNTs catalyst with cobalt significantly decreases the methanol selectivity and increases ethanol and other higher alcohols selectivities. The maximum higher alcohol selectivity of 41.65% (in liquid products) is observed over the catalyst with 3wt.% Co. Thus, cobalt not only promotes the activity and selectivity toward higher alcohols, but also propagates the chain growth mechanism leading to the formation of higher alcohols. The reason may be better explained from the XRD tests

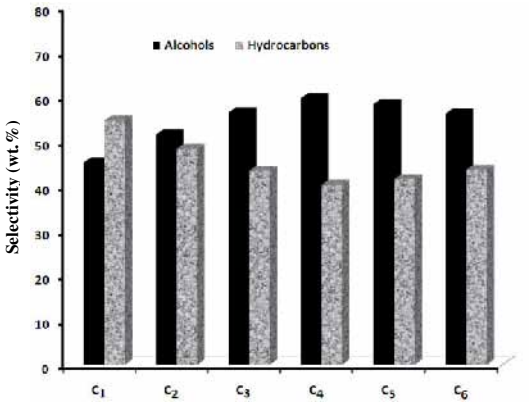

Fig. 6: Variations in the selectivity of alcohols and hydrocarbons in liquid products with Co loadings.

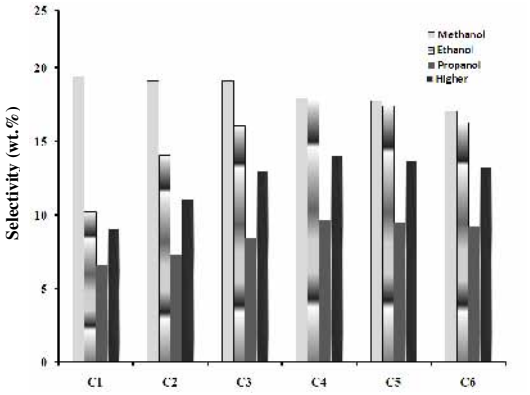

Fig. 7: Variations in the selectivity trends of individual alcohols with %Co loadings.

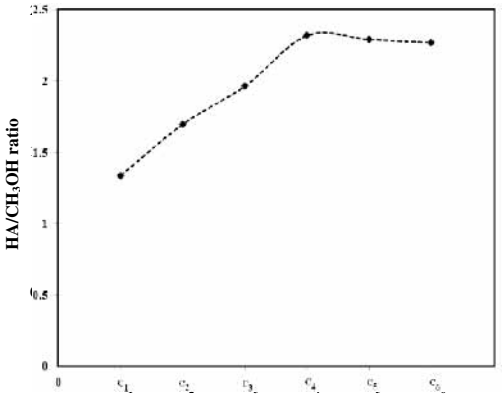

Fig. 8: Variations of HA/CH_3OH ratio with %Mo loadings.

with varying Co content. It is clear from XRD that the catalysts with 3wt.% Co showed larger K–Mo–O mixed oxides, which is responsible for privileged activity of these catalysts towards the formation of higher alcohols.

Fig. 8 show the variations of HA/CH_3OH ratio with increased Co loadings. In accordance with the results in Figs. 6 and 7, the catalyst with 3 wt.% Co shows highest ratio of higher alcohols to methanol production rate. Consequently, in higher alcohols selectivities point of view, 3 wt.% Co is the suitable loading.

CONCLUSIONS

Cobalt promoted alkalized MoS_2 catalysts supported on multi-wall carbon nanotubes are used to produce higher alcohols from synthesis gas. From the TEM images, it was found that metal species were uniformly distributed inside and outside of the tubes, with particle sizes in the range of 2 to 13 nm. Addition of cobalt decreased reduction temperature of the catalyst, increased the catalyst dispersion, decreased the average particle sizes from 7.53 to 5.31 nm and increased the chemical interactions between K–Mo–O species which enhance the formation of alcohols. Percentage conversion increased from 27.7 to 38.4 upon promotion of the catalyst with 5 wt.% cobalt. The total alcohol selectivity reached a maximum of 59.7 wt.% on the catalyst promoted with 3 wt.% cobalt. The catalyst with 3 wt.% Co exhibited selectivity of 41.65 wt.% towards higher alcohols.

Received : Apr. 13, 2012 ; Accepted : Oct. 15, 2012

REFERENCES

[1] Herman R., "Studies in Surface and Catalyst'', Chapter 7, Elsevier, Amsterdam, (1990).

[2] Johnston P., Hutchings G.J., Coville N.J., Finch K.P., Moss J.R., CO Hydrogenation Using Supported Iron Carbonyl Complexes, *Appl. Catal. A: General*, **186**(1-2), p. 245 (1999).

[3] Smith K.J., Anderson R.B., A Chain Growth Scheme for the Higher Alcohols Synthesis, *J. of Catalysis*, **85**, p. 428 (1984).

[4] Camposmartin J.M., Guerreroruiz A., Fierro J.L.G., Structural and Surface Properties of CuO-ZnO-Cr_2O_3 Catalysts and Their Relationship with Selectivity to Higher Alcohols Synthesis, *J Catal,* **156**(2), p. 208 (1995).

[5] Boz I., Sahibzada M., Metcalfe I.S., Kinetics of the Higher Alcohol Synthesis over a K-Promoted Cuo/Zno/Al2o3 Catalyst, *Ind Eng Chem Res*, **33**(9), p. 2021 (1994).

[6] Quarderer Q.J. et al., Catalytic Process for Producing Mixed Alcohols from Hydrogen and Carbon Monoxide, *PCT Int. Pat. Publication No*. WO84/03696 (1984).

[7] Kinkade N.E., Process for Producing Alcohols from Carbon Monoxide and Hydrogen Using an Alkali-Molybdenum Sulfide Catalyst, *PCT Int. Pat. Publication No. WO 85/03073* (1985).

[8] Jackson G.R. et al., Method for Production of Mixed Alcohols from Synthesis Gas, *U.S. Patent* 6,248,796 (2001).

[9] Chaumette P., Courty P., Durand D., Grandvallet P., Travers C., Process for Synthesizing a Mixture of Primary Alcohols from a Synthesis Gas in the Presence of a Catalyst Containing Copper, Cobalt, Zinc, and Aluminum, *GB Patent*, *2,158,730* (1985).

[10] Woo H.C., Park K.Y., Mixed Alcohol Using Molybdenum Carbide Catalysts, *Applied Catalysis*, **75**, p. 267 (1991).

[11] Jiang M., Bian G.-Z., Fu Y.-L., The Structure of Oxidic and Sulfided Mo Catalysts Supported on Activated Carbon was Studied by Means of X-Ray Diffraction, *J. of Catalysis*, **146**, p. 144 (1994).

[12] Lee J.S., Kim S., Lee K.H., Nam I.-S., Chung J.S., Kim Y.G., Woo H.C., Effect of the K-Mo Interaction in K-MoO_3/γ-Al_2O_3 Catalysts on the Properties for Alcohol Synthesis from Syngas, *Applied Catalysis*, **110**, p. 11 (1994).

[13] Tatsumi T., Muramatsu A., Yokota K., Tominga H., Mechanistic Study on the Alcohol Synthesis over Molybdenum Catalysts: Addition of Probe Molecules to CO-H_2, *J. of Catalysis*, **115**, p. 388 (1989).

[14] Iranmahboob J., Toghiani H., Hill D.O., Dispersion of Alkali on the Surface of Co-MoS_2/Clay Catalyst: a Comparison of K and Cs as a Promoter for Synthesis of Alcohol, *Applied Catalysis*, **247**, p. 207 (2003).

[15] Okamoto Y., Nakano H., Shimokawa T., Imanaka T., Teranishi S., Stabilization Effect of Co for Mo Phase in Co-Mo/Al_2O_3 hydrodesulfurization Catalysts Studied with X-Ray Photoelectron spectroscopy, *J. of Catalysis*, **50**, p. 447 (1977).

[16] Murchison C., Conway M., Steven R., Quarderer G., Proceedings of the 9th International Congress on Catalyst, **2**, p. 626 (1988).

[17] van Steen E., Prinsloo F.F., Comparison of Preparation Methods for Carbon Nanotubes Supported Iron Fischer-Tropsch Catalysts, *Catalysis Today*, **71**, p. 327 (2002).

[18] Surisetty V.R., Tavasoli A., Dalai A.K., Synthesis of Higher Alcohols from Syngas over Alkali Promoted MoS_2 Catalysts, *Applied Catalysis*, **365**, p. 243 (2009).

[19] Surisetty V.R., Dalai A.K., Kozinski J., Intrinsic Reaction Kinetics of Higher Alcohol Synthesis from Synthesis Gas Over a Sulfide Alkali-Ppromoted Co-Rh-Mo Trimetallic Catalyst Supported on MWCNTs, *Energy Fuels*, **24**, p. 4130 (2010).

[20] Surisetty V.R., Dalai A.K., Kozinski J., Influence of Porous Characteristics of the Carbon Support on Alkali-Modified Trimetallic Co-Rh-Mo Sulfided Catalysts for Higher Alcohols Synthesis from Synthesis gas, *Applied Catalysis*, **393**, p. 50 (2011).

[21] Surisetty V.R., Dalai A.K., Kozinski J., Effect of Rh Promoter on MWCNT-Supported Alkali-Modified MoS_2 Catalysts for Higher Alcohols Synthesis from CO Hydrogenation, *Applied Catalysis*, **381**, p. 282 (2010).

[22] Surisetty V.R., Dalai A.K., Kozinski J., Synthesis of Higher Alcohols from Synthesis Gas Over Co-Promoted Alkali-Modified MoS_2 Catalysts Supported on MWCNTs, *Applied Catalysis*, **358**, p. 153 (2010).

[23] Tavasoli A., Karimi S., Nikookar H., Fadakar H., Molybdenum Loading Effects on the Physico-chemical Properties and Performance of Carbon Nanotubes Supported Alkalized MoS_2 Catalysts for Higher Alcohols Synthesis, *Iran. J. Chem. & Chem. Eng.(IJCCE),* **32**(1) p. 1 (2012).

[24] Sun M., Nelsona A.E., Adjaye J., On The Incorporation of Nickel and Cobalt Iinto MoS_2-edge Structures, *J. of Catalysis*, **226**, p. 32 (2004).

[25] Topsøe H., Clausen B.S., Massoth F.E., Hydrotreating Catalysis, *Science and Technology*, **11**, p. 31 (1996).

[26] Tavasoli A., Sadaghiani K., Nakhaeipour A., Ahangari M.G., Cobalt Loading Effects on the Structure and Activity for Fischer-Tropsch and Water-Gas Shift Reactions of Co/Al_2O_3 Catalysts, *Iran. J. Chem. & Chem. Eng.(IJCCE),* **26**(4), p. 9 (2007).